# Synthesis and characterisation of oxygenated magnesium phthalocyanine

**ARTICLE** *in* POLYHEDRON · JUNE 2013

Impact Factor: 2.01 · DOI: 10.1016/j.poly.2013.03.065



**2 AUTHORS**, INCLUDING:

Jan Janczak
Polish Academy of Sciences
**264** PUBLICATIONS **2,782** CITATIONS

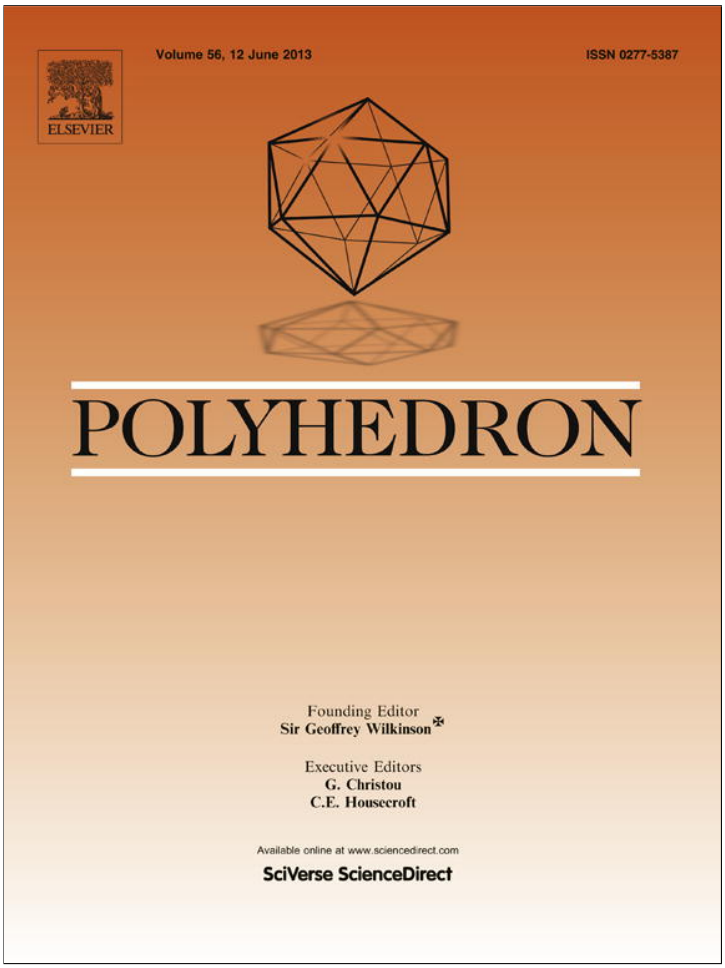

Polyhedron 56 (2013) 200–210

Contents lists available at SciVerse ScienceDirect

Polyhedron

journal homepage: www.elsevier.com/locate/poly

# Synthesis and characterisation of oxygenated magnesium phthalocyanine

Jan Janczak *, Ryszard Kubiak

*Institute of Low Temperature and Structure Research, Polish Academy of Sciences, Okólna 2 Str., P.O. Box 1410, 50-950 Wrocław, Poland*

ARTICLE INFO

*Article history:*
Received 20 February 2013
Accepted 25 March 2013
Available online 10 April 2013

*Keywords:*
Magnesium phthalocyanine
Oxygenated magnesium phthalocyanine
Crystal structure
DFT calculations
Molecular electrostatic potential

ABSTRACT

Two crystals of oxygenated magnesium phthalocyanine complex $(MgPc)_2O_2$ with a composition of $(MgPc)_2O_2{\cdot}2(MgPcDBU){\cdot}2DBU$ – crystal **1** (DBU = 1,8-diazabicyclo[5.4.0]undec-7-ene) and $(MgPc)_2O_2{\cdot}4(4\text{-Mepy})$ – crystal **2** were obtained. In both crystals the $(MgPc)_2O_2$ molecule is centrosymmetric and exhibits similar conformation, but different to that in the gas phase as obtained by DFT calculations. The Mg centre of both MgPc molecules of $(MgPc)_2O_2$ is 4+1 coordinated by four isoindole N atoms of Pc(2−) macrocycle in an equatorial position, and by oxygen atom of bridged dioxygen molecule in an axial position. Owing to the interaction of the electropositive Mg centre of MgPc molecules with the bridged dioxygen molecule, the Mg atom is significantly displaced (∼0.73 Å) from the plane defined by four isoindole N atoms of Pc(2−) macroring. In the MgPcDBU molecule in crystal **1** the interaction of Mg centre of MgPc with N atom of DBU in the axial position leads to the displacement of Mg from the $N_4$-plane by ∼0.63 Å. The interactions of Mg centre of MgPc with dioxygen molecule forming the oxygenated $(MgPc)_2O_2$ complex as well as the interactions of Mg centre of MgPc with N atom of DBU forming MgPcDBU complex lead a distortion of a planar Pc(2−) macrocycle to the saucer-shape form. The displacement of Mg from the $N_4$-plane as well as the distortion of Pc(2−) macrocycle from planar conformation is more pronounced in the crystals than that in the gas phase structure. Both crystals were also characterised by the thermal analysis. EPR and magnetic susceptibility measurement show the diamagnetic character (no net unpaired electrons) of oxygenated $(MgPc)_2O_2$ complex. The calculated three-dimensional MESP maps are helpful for understanding of the interactions between the MgPc and dioxygen molecule forming the oxygenated $(MgPc)_2O_2$ complex. The 3D MESP maps are also helpful for understanding the arrangement of molecules in a solid (crystal).



## 1. Introduction

Interest of magnesium phthalocyanine, MgPc where Pc = $C_{32}H_{16}N_8$, and its axially or biaxially ligated complexes, MgPcL and $MgPcL_2$ (L is a N or O donor ligand), arises from their similarity and relationship to chlorophyll (Scheme 1) and they can be used as its synthetic model [1,2].

Magnesium phthalocyanine similar to other metal(II) phthalocyaninato complexes (M(II)Pc) crystallises in two crystallographic modifications – α and β. However the single crystal structure has been determined only for β-modification [3]. Within the β-M(II)Pc complexes, the magnesium phthalocyanine is exceptional and unusual [4]. It has been stated that the crystals of MgPc are unstable in ambient atmosphere and absorb $O_2$ and/or $N_2$ forming complexes with the composition of $(MgPc)_2O_2$ and $(MgPc)_2N_2$ [5]. The formation of these complexes is reversible and strongly depends on the temperature. The instability of the β-MgPc crystals as well as its unusual and different behaviour in relation to other β-M(II)Pc arises from differences in their crystal structures. The X-ray single crystal structure analysis of MgPc shows that the Mg atom is, in contrast to other β-M(II)Pc complexes, significantly displaced from the $N_4$-isoindole plane (∼0.5 Å) and interacts with the N-azamethine atom of the neighbouring MgPc molecule [3]. Thus in the crystal the Mg atom of MgPc accommodates the 4+1 coordination. The differences in the crystal structure of MgPc, relatively to other β-M(II)Pc complexes, establish a chemical feature of MgPc that is responsible for its catalytic properties. For example the MgPc exhibits catalytic transformation of the cyano group(s) of organic cyano-compounds [6].

On the other hand the electrochemical properties of magnesium phthalocyanine and its 4+1 and 4+2 ligated complexes make them useful in several fields where phthalocyanines find applications. Due to their intense blue colour they are used as pigments in display devices, gas sensors, non-linear optics and solar cell conversion materials [7]. Several magnesium phthalocyaninato complexes, especially the sulphonated and alkyl or aryl-substituted derivatives are used as photosensitisers for photodynamic cancer therapy (PDT) due to their possibility to generate oxygen in the singlet state and their non-toxicity [8]. During photodynamic therapy with phthalocyanines as photosensitisers, they are first excited to the triplet state and then transfer the energy to

* Corresponding author. Tel.: +48 71 343 5021; fax: +48 71 344 1029.
*E-mail address:* j.janczak@int.pan.wroc.pl (J. Janczak).

0277-5387/$ - see front matter © 2013 Elsevier Ltd. All rights reserved.
http://dx.doi.org/10.1016/j.poly.2013.03.065

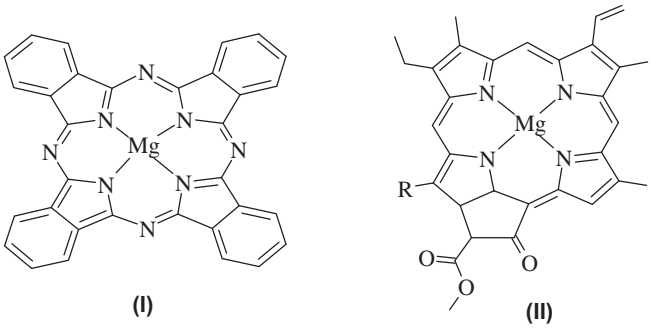


**Scheme 1.** The cChemical structures of magnesium phthalocyanine (**I**) and chlorophyll α (**II**).

the ground-state triplet oxygen ($O_2$, $^3\sum_g$), generating the excited-state singlet oxygen ($O_2$, $^1\Delta_g$). Their activities decrease in the order of ZnPc > MgPc > CuPc > MnPc > CoPc > FePc [9].

The molecular oxygen $O_2$ plays a great and significant role in many photobiological and photochemical processes such as photooxidation, photodegradation or photoaging [10]. It has been stated that chlorophyll α in benzene or in acetone in the presence of molecular oxygen was irreversibly bleached when exposed to visible light [11]. Ligation by $O_2$ is of interest because haeme and manganese porphyrins play central roles in the activation and transport of molecular oxygen $O_2$ in living organisms [12]. The photochemical reaction of chlorophyll α with molecular oxygen is especially interesting in its function during biochemical oxidation processes [13].

In this context, we used magnesium phthalocyanine as a synthetic model of chlorophyll, to investigate the interaction of molecular oxygen with MgPc and the formation of oxygenated magnesium phthalocyanine. The results will be helpful for understanding the nature of the interaction between the molecular oxygen and MgPc.

## 2. Experimental

### 2.1. Preparation of the oxygenated magnesium phthalocyanine complex from acetone – $(MgPc)_2O_2{\cdot}(MgPcDBU)_2{\cdot}2DBU$, (*1*)

Magnesium phthalocyanine and acetone were obtained from Sigma–Aldrich Co. and were used as received. The MgPc (1 g) was pressed into pellets and added into a glass ampoule containing 25 ml acetone. Then the ampoule was sealed under reduced pressure. Next the ampoule was heated at 270 °C for one day and then it was cooled to the room temperature. After such processing several well-developed single crystals **1** were grown on the surface of the pellets. The crystals **1** were separated under an optic microscope and some of them have been used for elemental analysis on an energy dispersive spectrometer as well as with a Perkin–Elmer 2400 elemental analyser. Calc. for $C_{164}H_{128}N_{40}O_2Mg_4$: Mg, 3.50; C, 70.54; N, 20.19; O, 1.34; H, 4.43. Found: Mg, 3.55; C, 70.48; N, 20.22; O, 1.33; H, 4.42%.

### 2.2. Preparation of the oxygenated magnesium phthalocyanine complex from 4-methylpyridine – $(MgPc)_2O_2{\cdot}4$(4-Mepy), (*2*)

The MgPc used in the reaction with 4-methylpyridine was obtained by the reaction of phthalonitrile and powder magnesium taken in the molar proportion of 4:1 according to the procedure described previously by us [3]. The freshly obtained single crystals of MgPc (~2 g) were added to 35 ml of 4-methylpyridine. The suspension was degassed and sealed in a glass ampoule and heated at 140 °C for one day. After such processing, the well-developed single crystals of $MgPc(H_2O){\cdot}$(4-Mepy) were obtained [14]. The $MgPc(H_2O){\cdot}$(4-Mepy) crystals were filtered washed with 4-methylpyridine, and the filtrate was left at ambient temperature in air. After several weeks in the filtrate, when almost all 4-methylpyridine was evaporated, the blue-violet well-developed single crystals **2** were formed. The obtained crystals of **2** were separated by filtration and washed with diethylether. The composition of the crystals obtained from 4-methylpyridine was checked with energy dispersive spectroscopy (EDS). EDS spectra were acquired and analysed using an EDAX Pegasus XM4 spectrometer with SDD Apollo 4D detector mounted on a FEI Nova NanoSEM 230 microscope. Calc. for $C_{88}H_{60}N_{20}O_2Mg_2$: Mg, 3.29; C, 71.50; N, 18.95; O, 2.17; H, 4.09. Found: Mg, 3.26; C, 70.25; N, 18.98 O, 2.32; H, 4.19%.

### 2.3. X-ray single crystal diffraction

Blue-violet single crystals of **1** and **2** were used for data collection on a four-circle KUMA KM4 diffractometer equipped with two-dimensional CCD area detector. The graphite monochromatised MoKα radiation ($\lambda$ = 0.71073 Å) and the $\omega$-scan technique ($\Delta\omega$ = 1°) were used for data collection. Data collection and reduction, along with absorption correction, were performed using CRYSALIS software package [15]. The structures were solved by direct methods using SHELXS-97 [16] revealing positions of almost all non-hydrogen atoms. The remaining atoms were located from subsequent difference Fourier syntheses. The structures were refined using SHELXL-97 [16] with the anisotropic thermal displacement parameters. The hydrogen atoms of the Pc and 4-Mepy were refined with a riding model, the hydrogen atoms of DBU molecule were constrained. The refinement of the crystal structure of **2** suggests the solvent accessible voids. The SQUEEZE procedure of the PLATON program [17] localises two positions at (0, 0, 0.004) and (0.5, 0.5, 0.255) with ~24 electrons in each for localisation of 4-Mepy molecule. However, the elemental analysis by TGA do not indicate any extra solvent, therefore the final refinement of **2** without SQUEEZE is presented in this work. Details of the data collection parameters, crystallographic data and final agreement parameters are collected in Table 1. Selected geometrical parameters are listed in Table 2. Visualisation of the structures was made with the DIAMOND 3.0 program [18].

### 2.4. Thermogravimetric measurements

Thermal analysis was carried out on a Linseis L81 thermobalance apparatus with Pt crucibles. The initial sample mass was about 20 mg. Powder $Al_2O_3$ was used as a reference. The measurements were performed under static air and recorded at the heating rate of 5 °C $min^{-1}$.

### 2.5. X-ray powder diffraction measurement

The rest of the sample left after thermogravimetric analysis was measured on a STOE diffractometer equipped with a linear PSD detector [19] using Cu $K\alpha_1$ radiation ($\lambda$ = 1.54060 Å) at room temperature.

### 2.6. EPR and magnetic susceptibility measurements

EPR measurements were carried out on SE-Radipan and ESP 300 E-Bruker X-band spectrometers at room temperature. The studies were performed on solid samples of 5–10 mg. Temperature dependence of the magnetic susceptibility was taken in the temperature range of 1.8–300 K with a Quantum Design SQUID magnetometer (San Diego, CA). Data were recorded at the magnetic field of 0.5 T on samples of 80–90 mg.

**Table 1**
Crystallographic data for oxygenated magnesium phthalocyanine complexes **1** and **2**.

| | **1** – $(MgPc)_2O_2\cdot 2(MgPcDBU)\cdot 2DBU$ | **2** – $(MgPc)_2O_2\cdot 4(4\text{-Mepy})$ |
|---|---|---|
| Formula | $C_{164}H_{128}N_{40}O_2Mg_4$ | $C_{88}H_{60}N_{20}O_2Mg_2$ |
| Molecular weight | 2788.30 | 1478.18 |
| Temperature | 295(2) | 295(2) |
| Crystal system | triclinic | monoclinic |
| Space group | $P\bar{1}$ (no. 2) | $C2/c$ (no. 15) |
| $a$ (Å) | 15.747(2) | 27.993(3) |
| $b$ (Å) | 18.230(3) | 17.376(2) |
| $c$ (Å) | 25.242(4) | 18.293(2) |
| $\alpha$ (°) | 79.710(10) | |
| $\beta$ (°) | 78.710(12) | 108.29(2) |
| $\gamma$ (°) | 83.480(11) | |
| $V$ (Å$^3$) | 6968.4(18) | 8448.3(19) |
| $Z$ | 2 | 4 |
| $D_{calc}$;/$D_{exp}$ (g cm$^{-1}$) | 1.329/1.32 | 1.162/1.16 |
| $\mu$ (mm$^{-1}$) | 0.1 | 0.087 |
| Crystal size (mm$^3$) | 0.33 × 0.28 × 0.19 | 0.37 × 0.32 × 0.25 |
| $T_{min}/T_{max}$ | 0.9694/0.9826 | 0.9697/0.9798 |
| Total/unique/Obs refls ($R_{int}$) | 69 062/30 278/15 221 (0.0805) | 42 835/9789/5522 (0.0656) |
| $R$ [$F^2 > 2\sigma(F^2)$][a] | 0.089 | 0.0749 [0.0725][*] |
| $wR$ [$F^2$ all refls][b] | 0.068 | 0.0720 [0.0708][*] |
| $S$ | 1.002 | 1.007 [1.004][*] |
| $\Delta\rho_{max}$, $\Delta\rho_{min}$ (e Å$^{-3}$) | 0.676, −0.603 | 0.195, −0.211 [0.237, −0.262][*] |

[a] $R = \Sigma\ ||F_o| - |F_c||/\Sigma F_o$.
[b] $wR = \{\Sigma[w(F_o^2 - F_c^2)^2]/\Sigma wF_o^4\}^{1/2}$; $w^{-1} = \sigma^2(F_o^2) + (aP)^2$ where $P = (F_o^2 + 2F_c^2)/3$. The $a$ parameter is 0.001 for **1** and 0.0065 for **2**.
[*] The SQUEEZED values are in square parentheses.

### 2.7. UV–Vis measurements

The electronic absorption spectra were carried out at room temperature using a Cary Varian SE UV–Vis–NIR spectrometer. The spectra of **1** and **2** were recorded in dichloromethane solution ($10^{-5}$ mol/l).

### 2.8. Theoretical calculations

Theoretical calculations with geometricaly optimisation of $(MgPc)_2O_2$ and MgPc(DBU) as well as the DBU and 4-methylpyridine, which are present in the crystals as a solvent, were performed with the GAUSSIAN03 program package [20]. All calculations were carried out with the DFT level using the Becke3-Lee-Yang-Parr correlation functional (B3LYP) [21,22] with the 3-21G basis set assuming the geometry resulting from the X-ray diffraction study as the starting structure. As convergence criterions the threshold limits of 0.00025 and 0.0012 a.u. were applied to the maximum force and the displacement, respectively.

## 3. Results and discussion

### 3.1. Synthesis and equilibrium in solution

The crystals of **1** were obtained from commercially available MgPc (Aldrich) from acetone. As has been shown by us, the O-donor ligands containing the lone electron pair at the O atom can interact with the electropositive Mg centre of MgPc forming O-axially ligated MgPc-derivatives [23]. Therefore, we expected that such thermal processing of MgPc in acetone as an O-ligand will also cause the formation of axially ligated MgPc-derivative with stoichiometry of MgPc to acetone equal to 1:1. However, the elemental analysis indicated that the composition of the obtained crystals **1** was different from that expected for the MgPc(acetone) complex. In addition, the X-ray single crystal determination shows unexpected, but interesting composition of the crystals, which are built up from two different MgPc-derivatives. One of them is monoaxially ligated by DBU MgPc-complex, and the second is oxygenated magnesium phthalocyanine, $(MgPc)_2O_2$. In addition both MgPc-derivatives co-crystallise with DBU as solvent molecule.

The axial coordination of the DBU molecule in the obtained crystals **1** can be understood, taking into consideration that the most frequently used method for synthesis of metallophthalocyanines is the cyclotetramerisation of phthalonitrile in the presence of a strong organic base such as DBU as a homogenous catalyst [24]. Therefore the commercially available MgPc dye (Aldrich, CAS No. 40,273-7) contains DBU as an impurity, and recrystallisation in acetone being a weaker base leads to formation of the MgPc–DBU complex. As has been shown by us, the β-MgPc crystals are unstable in ambient air and form complexes with $O_2$ [5]. Therefore, at used conditions, the molecular oxygen $O_2$ containing lone electron pair at both oxygen atoms can interact with the electropositive Mg centre of MgPc forming the oxygenated complex of $(MgPc)_2O_2$. Both MgPc-derivatives, i.e. MgPcDBU and $(MgPc)_2O_2$, co-crystallise with DBU as solvent molecules forming on the surface of the pellets' well-developed single crystals of **1**, i.e. $(MgPc)_2O_2\cdot 2MgPcDBU\cdot 2DBU$.

Since the commercially available MgPc dye contains DBU as impurity that was identified by TG and IR methods (Fig. S1a and b in Supplementary materials), the MgPc used in the reaction with 4-methylpyridine was obtained directly by the reaction of 1,2-dicyanobenzene and powder magnesium according to the procedure described previously by us [3]. The freshly obtained β-MgPc crystals were added to 4-Mepy. Recrystallisation of MgPc in 4-Mepy at 140 °C yields to $MgPc(H_2O)\cdot 4$-Mepy crystals that were separated by filtration and the filtrate was left at room temperature in ambient air. The $MgPc(H_2O)\cdot 4$-Mepy complex was characterised previously [14]. During slow evaporation of the solvent, after about three days in the filtrate the well-developed crystals are appeared. One of them has been checked on a KUMA KM-4 with CCD diffractometer and was affirmed it composition, $MgPc(H_2O)\cdot 2(4\text{-Mepy})\cdot 4$-Mepy, that has been characterised previously by us [14]. After about three days these crystals were dissolved in the mother filtrate forming a blue solution. Therefore, we suppose that the $MgPc(H_2O)\cdot 2(4\text{-Mepy})\cdot 4$-Mepy crystals

**Table 2**
Selected geometrical parameters (Å, °).

| $(MgPc)_2O_2$ | Molecule 1 | Molecule 2 | | *Ab initio* |
|---|---|---|---|---|
| *(a) $(MgPc)_2O_2$·2(MgPcDBU)·2DBU –* ***1*** | | | | |
| Mg11–N11 | 2.083(3) | Mg21–N21 | 2.090(3) | 2.052 |
| Mg11–N13 | 2.118(3) | Mg21–N23 | 2.058(4) | 2.057 |
| Mg11–N15 | 2.094(4) | Mg21–N25 | 2.111(3) | 2.061 |
| Mg11–N17 | 2.078(3) | Mg21–N27 | 2.086(4) | 2.057 |
| Mg11–O11 | 2.098(4) | Mg21–O21 | 2.116(4) | 2.033 |
| O11–O11$^{i}$ | 1.516(7) | O21–O21$^{ii}$ | 1.501(7) | 1.434 |
| N11–Mg11–N13 | 84.91(13) | N21–Mg21–N23 | 83.07(13) | 87.01 |
| N13–Mg11–N15 | 81.58(14) | N23–Mg21–N25 | 83.47(14) | 86.60 |
| N15–Mg11–N17 | 83.63(14) | N27–Mg21–N27 | 82.89(14) | 86.60 |
| N17–Mg11–N11 | 82.38(13) | N21–Mg21–N27 | 83.52(13) | 86.89 |
| N11–Mg11–O11 | 105.39(15) | N21–Mg21–O21 | 111.51(19) | 106.90 |
| N13–Mg11–O11 | 113.81(18) | N23–Mg21–O21 | 105.25(16) | 103.21 |
| N15–Mg11–O11 | 112.55(15) | N25–Mg21–O21 | 111.58(18) | 101.59 |
| N17–Mg11–O11 | 109.3(2) | N27–Mg21–O21 | 112.09(15) | 103.19 |
| Mg11–O11–O11$^{i}$ | 171.8(4) | Mg21–O21–O21$^{ii}$ | 171.5(4) | 98.10 |
| MgPcDBU | Molecule 1 | Molecule 2 | | |
| Mg31–N31 | 2.059(3) | Mg41–N41 | 2.074(3) | 2.067 |
| Mg31–N33 | 2.081(3) | Mg41–N43 | 2.066(4) | 2.068 |
| Mg31–N35 | 2.070(3) | Mg41–N45 | 2.071(3) | 2.069 |
| Mg31–N37 | 2.092(3) | Mg41–N47 | 2.083(4) | 2.069 |
| Mg31–N341 | 2.112(4) | Mg41–N441 | 2.083(3) | 2.140 |
| N31–Mg31–N33 | 83.30(14) | N41–Mg41–N43 | 83.89(14) | 86.70 |
| N33–Mg31–N35 | 85.05(13) | N43–Mg41–N45 | 85.11(14) | 86.29 |
| N35–Mg31–N37 | 84.71(13) | N45–Mg41–N47 | 85.17(14) | 86.60 |
| N37–Mg31–N31 | 85.81(14) | N47–Mg41–N41 | 84.37(13) | 86.30 |
| N31–Mg31–N341 | 110.87(14) | N41–Mg41–N441 | 105.83(14) | 107.19 |
| N33–Mg31–N341 | 102.60(14) | N43–Mg41–N441 | 112.95(15) | 99.51 |
| N35–Mg31–N341 | 104.74(15) | N45–Mg41–N441 | 110.78(14) | 101.20 |
| N37–Mg31–N341 | 112.16(15) | N47–Mg41–N441 | 101.45(15) | 109.19 |

Symmetry code: (*i*) $-x+1, -y+1, -z+1$; (*ii*) $-x+2, -y, -z$.

| | X-ray | DFT calculated |
|---|---|---|
| *(b) $(MgPc)_2O_2$·4(4-Mepy) –* ***2*** | | |
| Mg–N1 | 2.1227(19) | 2.052 |
| Mg–N3 | 2.0892(18) | 2.057 |
| Mg–N5 | 2.074(2) | 2.061 |
| Mg–N7 | 2.0964(18) | 2.057 |
| Mg–O | 2.0367(18) | 2.033 |
| O–O$^{i}$ | 1.556(4) | 1.434 |
| N1–Mg–N3 | 81.49(8) | 87.01 |
| N3–Mg–N5 | 83.33(7) | 86.60 |
| N5–Mg–N7 | 84.20(8) | 86.60 |
| N7–Mg–N1 | 82.83(8) | 86.89 |
| N1–Mg–O | 113.84(9) | 106.90 |
| N3–Mg–O | 117.26(7) | 103.21 |
| N5–Mg–O | 108.21(8) | 101.59 |
| N7–Mg–O | 102.52(8) | 103.19 |
| MgO$^{i}$–O–O$^{i}$ | 165.19(19) | 98.10 |

Symmetry code: (i) $-x+1/2, -y+1/2, -z$.

interact with the molecular oxygen forming oxygenated MgPc-supramolecular complex, which is well soluble in 4-Mepy as a mother liquid. After several weeks when the 4-Mepy partially evaporated, the concentration of the oxygenated MgPc complex increases, and in consequence the crystallisation process takes place. The formed crystals are oxygenated MgPc-complex that crystallises as 4-Mepy solvate as shown in the X-ray single crystal analysis.

### 3.2. Thermal stability

In order to determine the thermal stability of these complexes investigated here, the thermal analyses of **1** and **2** were carried out on the samples of 50 mg with the same heating rate of 5 °C/min. The thermogravimetric analyses of the solid-state samples are shown in Fig. 1. Crystal **1** is stable up to ~150 °C, and at higher temperature loses the solvated DBU molecules. After loss of the solvent DBU molecules, the starting compound transforms into $(MgPc)_2O_2$·2(MgPcDBU), which during further heating loses the

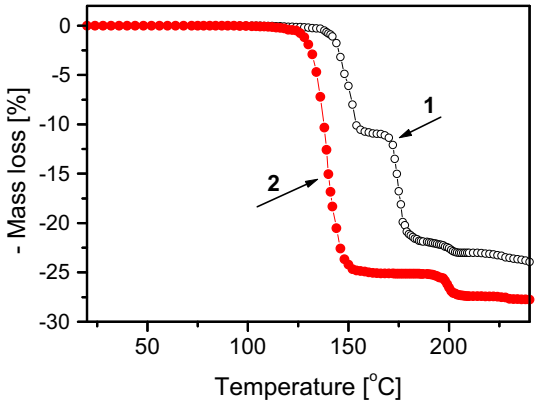


**Fig. 1.** Thermograms for the solid-state samples of **1** and **2**.

coordinated DBU molecules (at ~175 °C) and finally the dioxygen molecule at ~200 °C, and transforms into MgPc in the β-form that was confirmed by the X-ray powder diffraction experiment. The respective weight losses correspond well to the weight decrease by 10.91% due to release of the solvated DBU molecules (~150 °C), coordinated DBU molecule from MgPcDBU (~175 °C, 11.91%) and dioxygen molecule (~200 °C, 1.16%). The calculated total weight loss is equal to 22.99% and agrees well with the weight loss observed in the TG experiment (Fig. 1).

Crystal **2** loses its solvent 4-Mepy molecules at ~140 °C. After the loss of solvent 4-Mepy molecules the starting compound transforms into an oxygenated $(MgPc)_2O_2$ complex, which during further heating loses the bridging dioxygen molecule (~200 °C) and finally transforms into β-MgPc (confirmed by the X-ray powder diffraction experiment). The respective mass loss on the heating is ~25% (4-Mepy) and ~2.2% ($O_2$), and is in agreement with the calculated values of 25.10% and 2.27%, respectively.

The thermal decomposition of the crystals **1** and **2** correlates well with the strength of the Mg–O bonds in oxygenated $(MgPc)_2O_2$ molecule and with the strength of the axial Mg–N bond in MgPcDBU complex. The MgPcDBU complex with the axial Mg–N bond decomposes easier than the $(MgPc)_2O_2$ with the Mg–O bonds. Thus the releasing of the bridging $O_2$ molecule from the $(MgPc)_2O_2$ complex needs greater energy for the breaking of both Mg–O bonds than the energy for the breaking of the axial Mg–N bond in MgPcDBU complex. A similar correlation of the releasing of coordinating dioxane molecule from the bridged and non-bridged MgPc-complex is observed for $MgPc(dioxane)_2$·$(MgPc)_2$(dioxane) crystals [25].

### 3.3. Description of the structures

The crystals of **1** are built up from two different MgPc-complexes: oxygenated magnesium phthalocyanine $(MgPc)_2O_2$ and axially ligated by DBU magnesium phthalocyanine MgPcDBU. Both complexes co-crystallise with DBU as solvate molecules forming crystals with the composition of $(MgPc)_2O_2$·2(MgPcDBU)·2DBU. The asymmetric unit of **1** consists of two halves of $(MgPc)_2O_2$, two MgPcDBU molecules and two DBU molecules. Both centrosymmetric oxygenated $(MgPc)_2O_2$ molecules and both independent MgPcDBU molecules as well as both solvating DBU molecules exhibit quite similar conformation (Fig. S2, in Supplementary materials), therefore only one of them is illustrated in Fig. 2a–c. The $(MgPc)_2O_2$ complex is centrosymmetric, i.e. the inversion centre lies in the middle of the O–O bond. The electropositive Mg centre of two MgPc molecules interacts with electronegative oxygen atoms of molecular oxygen, containing the lone-electron pair, forming the oxygenated complex – $(MgPc)_2O_2$ (Fig. 2a). The Mg

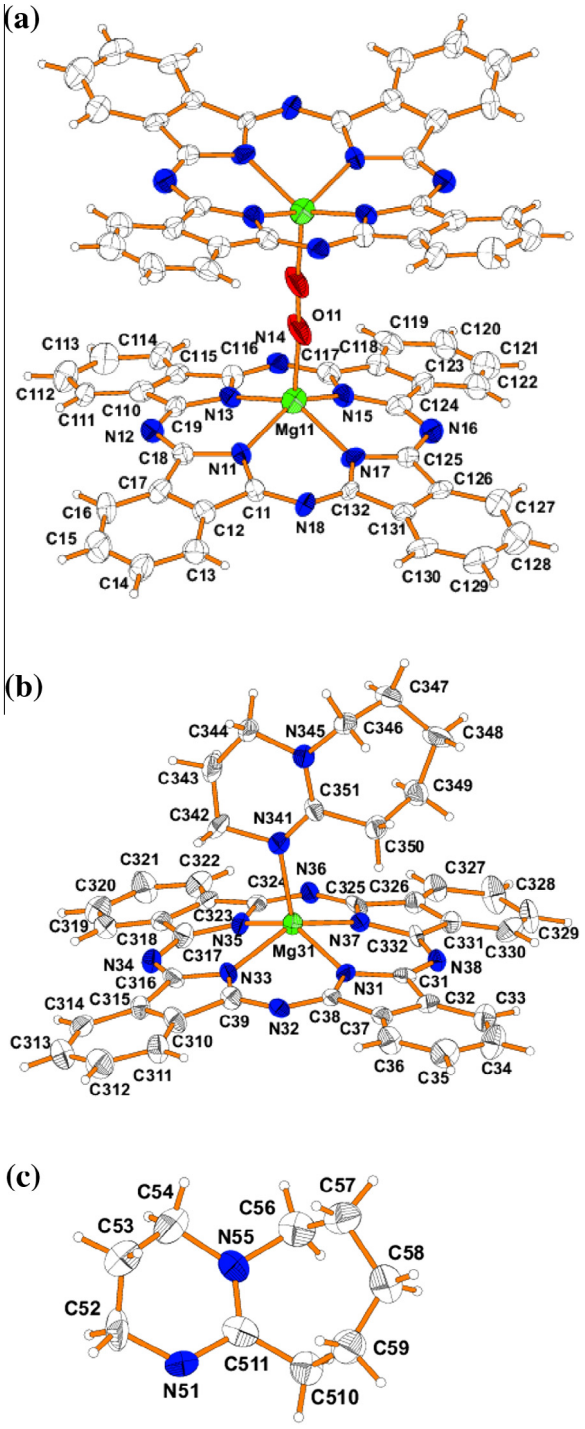


**Fig. 2.** View of the molecular structure of **1** showing only one of two independent molecules: $(MgPc)_2O_2$ (a), MgPcDBU (b) and DBU (c). Displacement ellipsoids are drawn at the 50% probability level.

atoms of $(MgPc)_2O_2$ are coordinated by four isoindole N atoms of phthalocyaninate(2−) macrocycle in the equatorial position and by oxygen atom of dioxygen molecule as a bridge forming H-shaped complex. Thus the Mg atoms exhibit 4+1 coordination. This coordination environment of the Mg atom is similar to that found in several chlorophyll derivatives [26], i.e. Mg is equatorially bound by four N atoms of pyrrole rings and by O atom in an axial position. Owing to the interaction of the electropositive Mg centre of MgPc molecules with the electronegative oxygen atoms of $O_2$ bridging molecules, in both centrosymmetric $(MgPc)_2O_2$ molecules, it is significantly displaced (0.726(3) and 0.718(3) Å) from the $N_4$-isoindole plane of the Pc(2−) macrocycle. The displacement of the Mg centre of MgPc from the $N_4$-plane in the oxygenated $(MgPc)_2O_2$ complex is about two times greater than that observed in the bridging by dioxane MgPc-complex (0.357(3) Å) [25]. The interaction between the electropositive Mg atom and the O atom of bridged dioxygen molecule in the H-shaped $(MgPc)_2O_2$ complex leads to the distortion of the Pc(2−) macrocycle from the $D_{4h}$ symmetry to the saucer-shape geometry. The four isoindole moieties are inclined to the $N_4$-plane of Pc(2−) by 14.02(2)°, 13.8(2)°, 8.2(2)° and 8.0(2)°, respectively for the N11C11–C18, N13C19–C119, N15C117–C124 and N17C125–C132 units. In the second $(MgPc)_2O_2$ molecule containing the Mg21 atom, the respective isoindole units are inclined to the $N_4$-plane by 16.1(2)°, 11.6(2)°, 8.9(2)° and 9.0(2)°. The four equatorial Mg–N bonds are comparable to the axial Mg–O bond with a bridging $O_2$ molecule. The relation between the equatorial Mg–N and axial Mg–O bonds in the oxygenated $(MgPc)_2O_2$ in crystal **1** is different from that in the bridged by dioxane MgPc-complex [25], but similar to that in the other 4+1 O-coordinated MgPc-derivatives, in which the axial Mg–O bond is comparable or even shorter than four equatorial Mg–N bonds [22]. The axial Mg–O bond is almost perpendicular to the $N_4$-plane, and the Mg11–O11–O11$^i$ (symmetry code: $i = 1 - x, 1 - y, 1 - z$) is equal to 171.9(2)°. The O–O distances of the bridging dioxygen molecule in both $(MgPc)_2O_2$ molecules in crystal **1** are not significantly different (1.516(7) Å in $(MgPc)_2O_2$ containing Mg11 and 1.501(7) Å in $(MgPc)_2O_2$ containing Mg21). These O–O distances are significantly elongated with respect to that observed for dioxygen molecule (∼1.25 Å) and very close to the oxygen-oxygen bond length observed for the systems containing peroxide dianion (∼1.49 Å). The value of O–O distance points on the presence of a peroxide dianion in the $(MgPc)_2O_2$ molecule. However, according to literature data the UV–Vis spectrum of the samples containing one-electron oxidised π-radical phthalocyanine ligand $Pc^{(-\cdot)}$ exhibits besides the Q and B bands one additional band around 450 nm [27], which is not present in our case (Fig. S3, in Supplementary materials). Both the Mg centre of MgPc molecules and the dioxygen molecule (Mg11–O11–O11$^i$–Mg11$^i$) are almost linear, and the Mg···Mg distance between the Mg centres is equal to 5.701(3) Å and 5.720(3) Å for $(MgPc)_2O_2$ molecules containing the Mg11 and Mg21, respectively. The distance between the $N_4$···$N_4$ planes in the $(MgPc)_2O_2$ molecules containing Mg11 and Mg21 is 7.119(3) and 7.130(3) Å, respectively.

The molecular structure of MgPcDBU molecule is illustrated in Fig. 2b. The central Mg atom of MgPc molecule exhibits 4+1 coordinative environment. The central Mg atom is equatorially bound to the phthalocyaninato(2−) macrocyclic ligand with a delocalised π system and to the ring nitrogen atom of DBU in the axial position. Owing to the interaction of the Mg with ring nitrogen atom of DBU it is significantly displaced (0.640(3) and 0.634(3) Å in MgPcDBU molecules containing Mg31 and Mg41 atoms, respectively) from the plane defined by the four isoindole N atoms of Pc macrocycle. The planar phthalocyaninate(2−) macrocycle of MgPc upon ligation by DBU adopts the saucer-shape form due to the interaction of the electropositive Mg centre of MgPc with ring nitrogen atom containing the lone electron pair of axial DBU molecule. The isoindole moieties of phthalocyaninate(2−) macrocycle are inclined by 8.1(2)–12.9(2)° and 7.4(2)–12.9(2)° to the $N_4$-plane in both independent MgPcDBU molecules containing the Mg31 and Mg41, respectively. The four equatorial Mg–N bonds in both independent MgPcDBU molecules are shorter than the axial Mg–N bond linking the DBU molecule (Table 2). A similar correlation between the equatorial and axial Mg–N bonds is observed in the 4+1 coordinated by DBU molecule ZnPc-derivative [28].

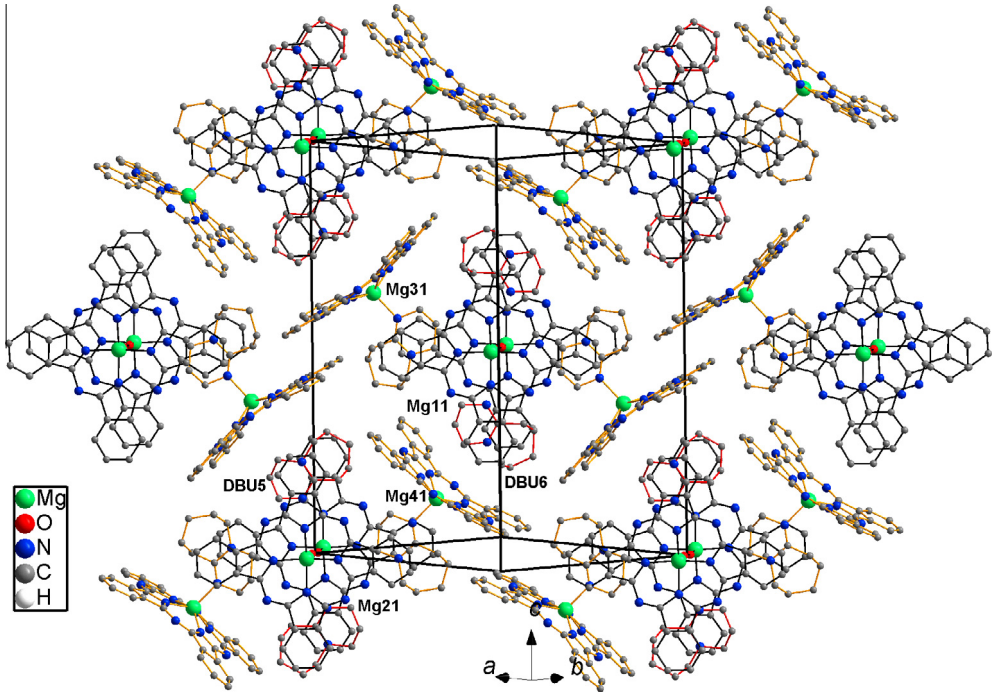


**Fig. 3.** Arrangement of $(MgPc)_2O_2$, MgPcDBU and DBU molecules in the unit cell showing the interpenetration of each isoindole units in $(MgPc)_2O_2$ by coordinated (orange MgPcDBU) and solvated DBU (red) molecules.

The mutual arrangement of $(MgPc)_2O_2$, MgPcDBU and DBU molecules in the crystal is illustrated in Fig. 3. The centre of O–O bond of bridged dioxygen molecule of both independent $(MgPc)_2O_2$ molecules lies in the inversion centre, thus the $(MgPc)_2O_2$ molecules are centrosymmetric. The DBU molecules (solvated or coordinated from MgPcDBU) interpenetrate each pair of isoindole units of the $(MgPc)_2O_2$ molecule, since the distance between the Pc(2−) macrocycles in the $(MgPc)_2O_2$ molecule is big enough, forming a $(MgPc)_2O_2{\cdot}2(MgPcDBU){\cdot}2(DBU)$ centrosymmetric cluster. These clusters are arranged into a two-dimensional layer parallel to the (1 1 0) plane, which is illustrated in Fig. 3.

The molecular structure of oxygenated magnesium phthalocyanine in crystal **2** (Fig. 4) exhibits quite similar conformation as that in crystal **1**. The $(MgPc)_2O_2$ complex in **2**, similar as in **1**, is centrosymmetric, i.e. the inversion centre lies on the centre of O–O of bridged dioxygen molecule. The respective geometrical parameters (bond lengths and angles) of $(MgPc)_2O_2$ molecule in **2** are similar to that as in crystal **1** (Table 2). The Mg atom is displaced from the $N_4$-plane by 0.734(3) Å. The inclination of the isoindole units of Pc(2−) macrocycles to the $N_4$-plane is smaller to that in crystal **1**. Additionally, the $N_4$–$N_4$ distance between the Pc(2−) macrocycles is shorter by ~0.15 Å than that in crystal **1**. The shorter $N_4$–$N_4$ distance and smaller inclination of the isoindole units in $(MgPc)_2O_2$ molecule in crystal **2** comparing to **1** result from different molecules located between each pairs of isoindole units of the $(MgPc)_2O_2$ system, i.e. 4-Mepy in **2** and DBU (solvated or coordinated) in **1** (see Figs. 3 and 4).

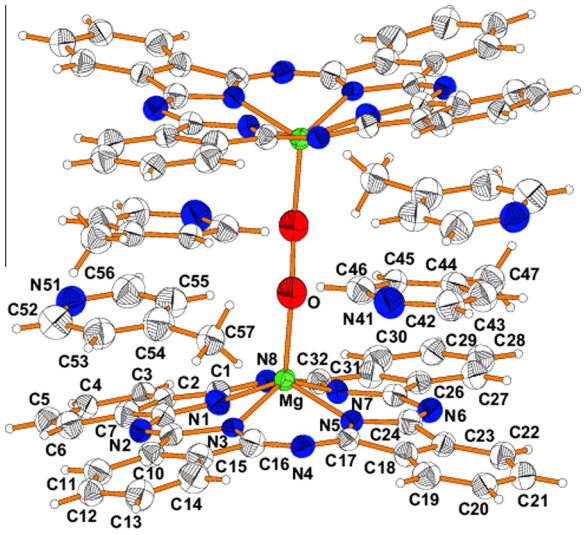


**Fig. 4.** View of the molecular structure of **2**. Displacement ellipsoids are drawn at the 50% probability level.

The mutual arrangement of centrosymmetric $(MgPc)_2O_2{\cdot}4$(4-Mepy) molecules in the crystal **2** (Fig. 5) is different from the arrangement of $(MgPc)_2O_2$ in **1**. In crystal **1** the $(MgPc)_2O_2$ molecules are form layers in which all Pc(2−) macrorings are parallel, whereas in **2** the $(MgPc)_2O_2$ molecules form layers, in which each $(MgPc)_2O_2$ molecule is rotated by 90° in relation to the neighbour (Fig. 5).

### 3.4. Gas phase structure

The gas-phase geometries of the oxygenated $(MgPc)_2O_2$ and MgPcDBU complexes were obtained by DFT calculations starting from the geometry obtained from the X-ray structure. The bond lengths and angles of the optimised gas-phase conformation of the $(MgPc)_2O_2$, in general, are in good agreement with those obtained from the X-ray structure determinations (Table 2). However, the gas-phase conformation of the $(MgPc)_2O_2$ (see Fig. 6) is different than that in the crystals **1** and **2**. Noticeable differences between the X-ray and DFT results in the coordination environment of the Mg atoms are observed. The displacement of the Mg centre of MgPc of centrosymmetric $(MgPc)_2O_2$ molecule from the $N_4$-plane is significantly smaller (by ~50%) than that in the crystals (Table 3). Other large differences between X-ray and DFT results

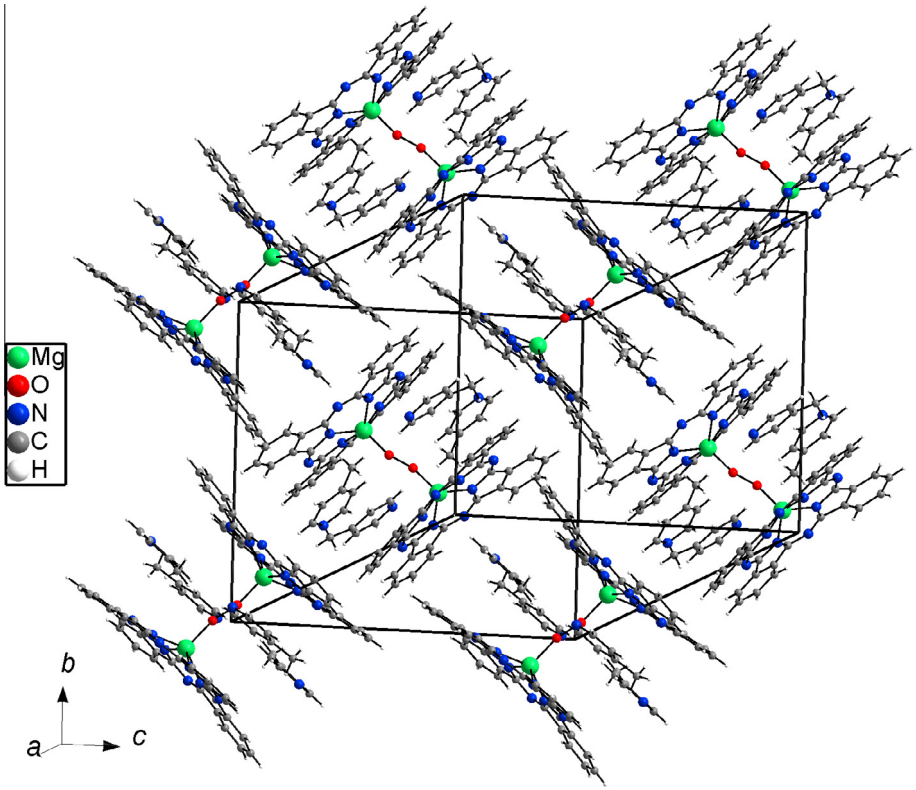


**Fig. 5.** Arrangement of $(MgPc)_2O_2{\cdot}4$(4-Mepy) showing the interpenetration of each isoindole units in $(MgPc)_2O_2$ by solvated 4-Mepy molecules.

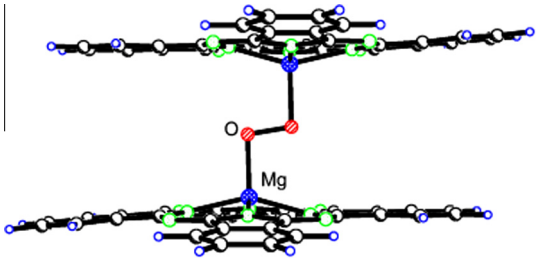


**Fig. 6.** View of the ab-initio structure of oxygenated magnesium phthalocyanine $(MgPc)_2O_2$.

are observed in the Mg–O–O angle and in the $N_4{\cdots}N_4$ distance between the Pc(2−) macrorings in the $(MgPc)_2O_2$ complex. The Mg–O–O angle is 98.1° and the $N_4{\cdots}N_4$ distance is 5.300 Å, these DFT values are different than that in the crystals, in which Mg–O–O angle is almost linear and the $N_4{\cdots}N_4$ distance significantly longer (Table 3). The changing of the Mg–O–O angle in DFT optimised conformation of $(MgPc)_2O_2$ molecule from 98.1° to ~171° upon crystallisation yielding crystal **1** or ~165° in crystal **2** results from the interaction and interpenetration of the DBU molecules (from MgPcDBU or solvated DBU in **1**) or 4-Mepy (in **2**) between each pairs of isoindole moieties of $(MgPc)_2O_2$ system (Figs. 3 and 5). Increasing of the Mg–O–O angle of $(MgPc)_2O_2$ molecule in crystal **1** is greater than in crystal **2** and correlate well with the dimensions of the interpenetrating molecules (non-planar DBU in **1** and planar 4-Mepy in **2**). In DFT optimised conformation of $(MgPc)_2O_2$ molecule the Mg–O–O angle as expected is smaller than 109.5° since the lone electron pairs at the O atoms afford a wider region than the bonding pair and is in agreement with the valence-shell-electron-pair repulsion model [29]. Additionally, the DFT optimised saucer shape geometry of Pc(2−) macrorings is less pronounced than that in the crystals. These differences result from the interactions between the Pc(2−) macrorings and the DBU molecules (solvated or coordinated MgPcDBU) in crystal **1** or between Pc(2−) macrorings and 4-Mepy molecules in crystal **2**, in which between each pairs of isoindole moieties is located the DBU (in **1**) or 4-Mepy molecule (in **2**). In crystals the interpenetration of DBU (or 4-Mepy) between each pair of isoindole units in $(MgPc)_2O_2$ supramolecule leads to elongation of the O–O in the bridged dioxygen molecule and to increasing of the displacement of Mg from the $N_4$-plane and to greater deviations of Pc(2−) macrocycles from planarity, so their saucer shape geometries in crystals are more pronounced than that in the gas-phase. The interactions of the molecules (DBU or 4-Mepy) and isoindole units of Pc(2−) macrocycles make the Mg–O–O angles almost linear (Table 3).

The gas-phase geometry of MgPcDBU molecule is very similar to that in the crystal. The difference between the energies of optimised geometry and that in the crystal is ~15.95 kJ $mol^{-1}$. The DFT geometrical parameters are, in general, in good agreement with those obtained from the X-ray structure analysis (Table 2). However, noticeable differences between the coordination environments of Mg atom are observed (Table 4). The optimised value of the axial Mg–N bond is slightly longer than the X-ray value, however the relation between the equatorial Mg–N and the axial Mg–N bonds is preserved as in the crystal. The displacement of Mg from the $N_4$-plane is smaller than that in the crystal. The saucer shape geometry of the Pc(2−) macrocycle in the gas-phase MgPcDBU molecule is less pronounced that that in the crystal (Table 4), which results from the intermolecular interaction and the crystal packing.

### 3.5. Magnetic properties

In order to determine the nature of the interaction of molecular oxygen $O_2$ with two MgPc molecules with the formation of an

**Table 3**
Comparison of selected conformational parameters (Å, °) of oxygenated $(MgPc)_2O_2$ complex in the gas-phase and in the crystals.

| | DFT | X-ray | | |
|---|---|---|---|---|
| | | **1** Molecule Mg11 and Mg21 | | **2** |
| Average Mg–N | 2.057 | 2.093 | 2.086 | 2.097 |
| Axial Mg–O | 2.033 | 2.098(4) | 2.116(4) | 2.037(2) |
| Displacement of Mg from the $N_4$-plane | 0.489 | 0.723(3) | 0.718(3) | 0.734(3) |
| Distance $N_4$–$N_4$ | 5.300 | 7.119(4) | 7.130(3) | 6.973(3) |
| Angle Mg–O–O | 98.1 | 171.8(4) | 171.5(4) | 165.19(19) |
| O11–O11$^i$ | 1.434 | 1.516(7) | 1.501(7) | 1.556(4) |
| *Dihedral angle between the $N_4$-plane and the isoindole units* | | | | |
| $N_4$/N11C11–C18 | 1.7 | 14.0 | 11.6 | 10.6 |
| $N_4$/N13C19–C116 | 6.8 | 13.8 | 16.1 | 7.8 |
| $N_4$/N15C117–C124 | 6.1 | 8.2 | 8.9 | 11.5 |
| $N_4$/N17C125–C132 | 6.8 | 8.0 | 9.0 | 1.8 |

**Table 4**
Comparison of coordination environment of Mg (Å, °) in MgPcDBU complex in the gas-phse and in the crystals.

| | DFT | X-ray Molecule Mg31 and Mg41 | |
|---|---|---|---|
| Average of equatorial Mg–N | 2.067 | 2.075 | 2.073 |
| Axial Mg–N | 2.140 | 2.112(4) | 2.083(3) |
| Displacement of Mg from the $N_4$-plane | 0.511 | 0.630(3) | 0.634(3) |
| *Dihedral angle between the $N_4$-plane and the isoindole units* | | | |
| $N_4$/N31C31–C38 | 6.9 | 8.1(2) | 7.4(2) |
| $N_4$/N33C39–C316 | 6.2 | 11.4(2) | 12.9(2) |
| $N_4$/N35C317–C324 | 6.9 | 10.9(2) | 10.5(2) |
| $N_4$/N37C325–C332 | 7.3 | 12.9(2) | 12.8(2) |

**Table 5**
Selected Milliken charges.

| Atom | MgPc | $O_2$ | DBU | 4-Mepy | $(MgPc)_2O_2$ | MgPcDBU |
|---|---|---|---|---|---|---|
| Mg | 1.076 | | | | 1.004 | 1.038 |
| O | | 0.0 | | | −0.218 | |
| $N_{azamethine}$ | −0.676 | | | | −0.677 | −0.680 |
| $N_{isoindole}$ | −0.791 | | | | −0.750 | −0.749 |
| Pyridine N-ring | | | | −0.186 | | |
| N in DBU[a] | | | −0.253 | | | −0.644 |
| N in DBU[b] | | | −0.068 | | | −0.651 |

[a] N of six-membered ring.
[b] N tertiary.

oxygenated $(MgPc)_2O_2$ complex, the EPR and magnetic susceptibility measurements on a solid state sample of **1** and **2** have been performed. The EPR measurements showed no resonance signal. The magnetic susceptibility experiments on **1** and **2** performed in the temperature range of 1.8–300 K showed their diamagnetic character (Fig. S4, in Supplementary materials). Thus both EPR and magnetic susceptibility experiments have shown the diamagnetic (no net unpaired electrons) character of the oxygenated $(MgPc)_2O_2$ complex.

These experiments point to the three logical possibilities to produce diamagnetic, no net spin, $(MgPc)_2O_2$ complex. (1) Two MgPc molecules are bridged by the singlet oxygen molecule ($O_2$, $^1\Delta_g$), since the MgPc and the singlet oxygen molecules are diamagnetic. However, the singlet oxygen is the higher-energy form of $O_2$ molecule. The energy difference between the energy of $O_2$ in the singlet state and the energy of $O_2$ in the triplet state, which is the ground state of dioxygen molecule, is ~98.3 kJ mol$^{-1}$ [30]. (2) The superoxide ion $O_2^-$ with unpaired electron bridges MgPc molecule and one electron oxidised π-radical $[MgPc^{(-\cdot)}]^+$ unit with the unpaired electron on the phthalocyaninate(−**·**) ring, the unpaired electrons couple antiferromagnetically giving the diamagnetic properties. (3) The dimagnetic peroxide ion $O_2^{2-}$ bridges two MgPc molecules, both one electron oxidised π-radical $[MgPc^{(-\cdot)}]^+$ units. The unpaired electrons on both $[MgPc^{(-\cdot)}]^+$ units of $(MgPc)_2O_2$ molecule couple antiferromagnetically giving diamagnetic properties.

### 3.6. Molecular electrostatic potential

The electrostatic potential $V(r)$ that the electrons or nuclei of a molecule create at each point $r$ in the surrounding space can be calculated by the equation $V(r) = \sum_A(Z_A/(R_A - r)) - \int(\rho(r')/|r' - r|)dr$, where $Z_A$ is the charge on nucleus A having a position vector $R_A$ and the $\rho(r')$ is the electron density function of the molecule. The molecular electrostatic potential (MESP) carry a wealthy quantitative and qualitative information and is widely used as a reactivity map displaying the most probable regions of molecule for the electrophilic attack of reagents. The MESP maps have emerged as powerful predictive and interpretative tools in several fields of chemistry, biology and the crystal engineering, for example rational drug design, catalysis, nucleophilic reaction and intermolecular interactions and organisation of molecules in solids [31]. The MESP carry the information about the distribution of the charge of the interacting molecules. The Milliken charges were calculated for each atoms of molecules (reacting molecules and the final products) and the selected values are summarised in Table 5.

The three-dimensional MESP maps are obtained on the basis of the DFT (B3LYP) optimised geometries of molecules. The calculated 3D MESP is mapped onto the total electron density isosurface (0.008 e Å$^{-3}$) for each molecules (Fig. 7). The colour code of MESP is in the range of −0.05 (red) to 0.05 e Å$^{-1}$ (blue). Regions of negative MESP are usually associated with the lone pair of electronegative atoms (O and N), whereas the regions of positive MESP are associated with the electropositive atoms.

For MgPc molecule the calculated 3D MESP map displays the electrophilic region near the Mg centre on both side of the planar MgPc molecule and the nucleophilic regions near the bridged azamethine nitrogen atoms (Fig. 7a). In addition, the less positive value of MESP than that near the Mg centre and the less negative value of MESP comparing to that of azamethine N bridges are observed across the extended 18 π-electron conjugation in the Pc macrocycle and on the both side of the phenyl rings, respectively. The calculated 3D MESP map of MgPc will be helpful for understanding its interaction with dioxygen molecule forming the oxygenated $(MgPc)_2O_2$ complex as well as the interaction of MgPc with DBU forming MgPcDBU complex.

The 3D MESP maps were calculated also for dioxygen molecule in the triplet ground state (Fig. 7b) and singlet excited state

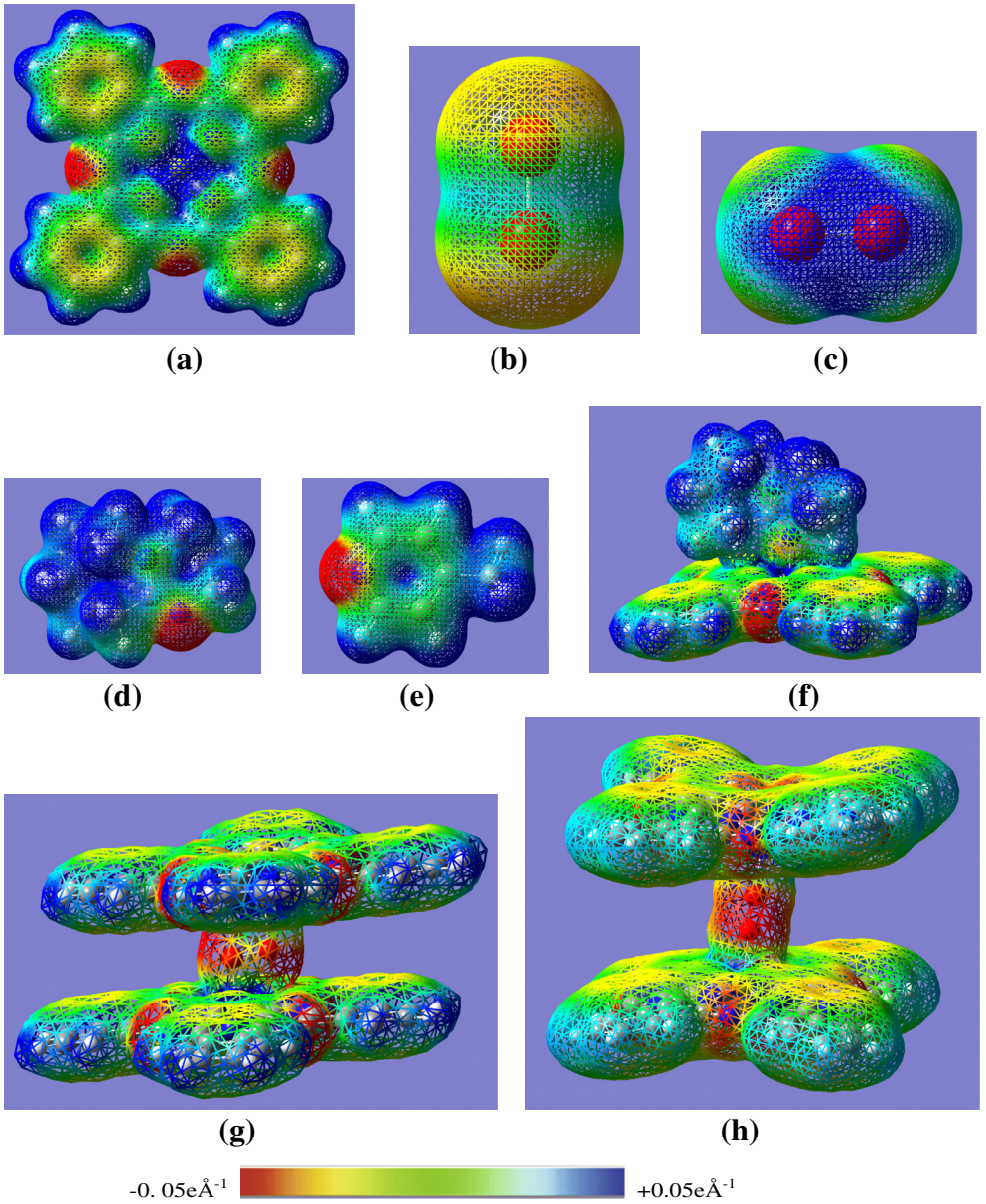


**Fig. 7.** Three-dimensional molecular electrostatic potential (−0.05 e Å$^{-1}$, red and +0.05 e Å$^{-1}$, blue) mapped on the surface of total electron density (0.008 e Å$^{-3}$) for the molecules: MgPc (a), $O_2$ ($^3\sum_g$) (b), $O_2$ ($^1\Delta_g$) (c), DBU (d), 4-Mepy (e), MgPcDBU (f), $(MgPc)_2O_2$ in the gas phase conformation (g) and $(MgPc)_2O_2$ in the crystal conformation (h).

(Fig. 7c), DBU (Fig. 7d), 4-Mepy (Fig. 7e) and MgPcDBU (Fig. 7f), since they are present in the investigated crystals **1** and **2** as co-crystallisation or solvent molecules. The interaction of MgPc and dioxygen molecule $O_2$ yielding $(MgPc)_2O_2$ complex or the interaction of MgPc with DBU yielding MgPcDBU complex can be understood. The interaction between the MgPc molecules and the oxygen atom of bridged dioxygen molecule takes place between the electropositive Mg centre of MgPc (blue colour, in Fig 7a) and the electronegative region of $O_2$ (red-orange, Fig. 7b and c) forming $(MgPc)_2O_2$ complex with Mg ← O coordinating bonds (Fig. 7g and h), whereas interaction between the MgPc and DBU takes place between the electropositive Mg centre of MgPc and the electronegative secondary N atom of DBU (Fig. 7d) forming MgPcDBU complex with Mg ← N coordinating bond (Fig. 7f). Since the conformation of $(MgPc)_2O_2$ complex in the gas-phase and in the crystal is different, the three dimensional MESP for $(MgPc)_2O_2$ supramolecule was calculated for both conformations, the gas phase conformation and the conformation present in the crystal, and the results are illustrated in Fig. 7g and h, respectively.

The arrangement of $(MgPc)_2O_2$, MgPcDBU and DBU molecules in the crystal **1** and $(MgPc)_2O_2$ and 4-Mepy molecules in the crystal **2** can be understood if we take into account their molecular electrostatic potential maps. In **1**, each pair of isoindole units of the $(MgPc)_2O_2$ molecule is separated by the solvent or coordinated DBU molecules (MgPcDBU) and in **2**, each pair of isoindole units of the $(MgPc)_2O_2$ molecule is separated by the solvent 4-Mepy molecules. The interaction between isoindole units of $(MgPc)_2O_2$ molecule with slightly negative values of MESP and DBU molecule (solvated or coordinated) with the electropositive values of MESP in **1** leads to stabilisation of the structure. In **2**, the interaction between the isoindole units of $(MgPc)_2O_2$ and the 4-Mepy leads to the π–π stabilisation of the structure.

## 4. Conclusions

In this work, we have described the synthesis and characterisation of oxygenated magnesium phthalocyanine $(MgPc)_2O_2$ complex. The $(MgPc)_2O_2$, depending on the conditions

used, co-crystallises as $(MgPc)_2O_2{\cdot}(MgPcDBU)_2{\cdot}2DBU$ (**1**) or $(MgPc)_2O_2{\cdot}4$(4-Mepy) (**2**). The molecular oxygen $O_2$ ($^3\sum_g$) interacts with two MgPc molecules forming diamagnetic oxygenated magnesium phthalocyanine $(MgPc)_2O_2$ (EPR and magnetic susceptibility experiments shown no-net unpaired electrons). There are three possibilities to produce the diamagnetic $(MgPc)_2O_2$ complex: (1) two MgPc molecules are bridged by the singlet $O_2$ ($^1\Delta_g$); (2) the superoxide $O_2^-$ with unpaired electron bridges MgPc and one electron oxidised π-radical $[Mg^{(2+)}Pc^{(-\cdot)}]^+$ cationic unit and (3) diamagnetic peroxide ion $O_2^{2-}$ bridges two MgPc molecules, both one electron oxidised π-radical $[Mg^{(2+)}Pc^{(-\cdot)}]^+$ units. The unpaired electrons couple antiferromagnetically giving diamagnetic character. The structural features strongly suggest the μ-peroxo electronic structure of dioxygen moiety and the diamagnetic character of the $(MgPc)_2O_2$ complex results from the strong magnetic exchange (spin quenching) between the π-radical $[Mg^{(2+)}Pc^{(-\cdot)}]^+$ subunits. The non-toxicity of oxygenated magnesium phthalocyanine complex makes its useful as a potential photosensitiser for photodynamic therapy of cancer.

## Acknowledgements

This work was supported by the Ministry of Science and Higher Education (grant No. N N204 397540). Special thanks to Dr. M. Hoffmann from A. Mickiewicz University of Poznań for the opportunity to make the MESP maps with the GAUSSVIEW program in his laboratory.

## Appendix A. Supplementary data

CCDC 899997 and 899996 contain the supplementary crystallographic data for **1** and **2**. These data can be obtained free of charge via http://www.ccdc.cam.ac.uk/conts/retrieving.html, or from the Cambridge Crystallographic Data Centre, 12 Union Road, Cambridge CB2 1EZ, UK; fax: +44 1223 336 033; or e-mail: deposit@ccdc.cam.ac.uk. Supplementary data (thermogram for a commercially available MgPc sample, the IR spectrum of a liquid obtained during thermal processing of commercially available MgPc, UV–Vis, plots of $\chi_M T$ vs $T$ for crystal **1** and **2**. Details on data collection and refinement, fractional atomic coordinates, anisotropic displacement parameters and full list of bond lengths and angles in CIF format) associated with this article can be found, in the online version, at http://dx.doi.org/10.1016/j.poly.2013.03.065.

## References

[1] R.K. Clayton, in: L.P. Vernon, G.R. Seely (Eds.), The Chlorophyll, Academic Press, New York, 1975.
[2] N.B. McKeown, Phthalocyanine Materials: Synthesis, Structure and Function, Cambridge University Press, Cambridge, 1998.
[3] J. Janczak, R. Kubiak, Polyhedron 20 (2001) 2901.
[4] A.T. Davidson, J. Chem. Phys. 245 (1982) 168.
[5] R. Kubiak, J. Janczak, K. Ejsmont, Chem. Phys. Lett. 245 (1995) 249.
[6] (a) J. Janczak, R. Kubiak, Acta Chem. Scand. 53 (1999) 602;
(b) J. Janczak, M. Śledź, R. Kubiak, J. Mol. Struct. 659 (2003) 71;
(c) J. Janczak, R. Kubiak, Acta Crystallogr., Sect. C 59 (2003) o506;
(d) J. Janczak, Polyhedron 38 (2012) 75.
[7] (a) R.O. Loutfy, A.M. Hor, G. DiPaola-Barnyi, C.K. Hsiao, J. Imaging Sci. 29 (1985) 116;
(b) W. Herbst, K. Hunger, Industrial Organic Pigments, VCH, New York, 1993;
(c) M. Yamashita, F. Inui, K. Irokawa, A. Moriugawa, T. Takao, M. Mito, H. Moriwaki, Appl. Surf. Sci. 883 (1998) 130;
(d) K.Y. Law, Chem. Rev. 93 (1993) 449;
(e) P.A. Lane, J. Rostalski, C. Giebeler, S.J. Martin, D.D.C. Bradley, D. Meissner, Solar Energy Mater. Sol. Cells 63 (2000) 3;
(f) G.A. Rosquete-Pina, C. Zorilla, S. Velumani, J. Arenas-Alatorre, J.A. Ascencio, Appl. Phys. A 79 (2004) 1913;
(g) R. Ao, L. Kilmmert, D. Haarer, Adv. Mater. 7 (1995) 495;
(h) B. Brożek-Płuska, W. Czajkowski, M. Kurczewska, H. Abramczyk, J. Mol. Liq. 141 (2008) 140.
[8] (a) R. Bonnett, Chemical Aspects of Photodynamic Theraphy, Gordon and Breach, Amsteldijk, Netherlands, 2000. p. 199;
(b) A. Paul, A. Mölich, S. Oelckers, M. Seifert, B. Röder, J. Porphyrins Phthalocyanines 6 (2002) 340;
(c) J.D. Spikes, Photochem. Photobiol. 43 (1986) 691;
(d) H. Weitman, S. Shatz, B. Ehrenberg, J. Photochem. Photobiol. A: Chem. 203 (2009) 7;
(e) R. Cubeddu, Gi. Ganti, C.D. Andrea, A. Pifferi, P. Taroni, A. Torricelli, G. Valentini, J. Photochem. Photobiol. B: Biol. 60 (2001) 73;
(f) A.V. Lobanov, G.I. Kobzev, K.S. Davydov, L.V. Koumaneikina, G.G. Komissarova, Macroheterocycles 4 (2011) 106;
(g) I. Lanzo, N. Russo, E. Sicilia, J. Phys. Chem. B 112 (2008) 4123;
(h) K. Ishii, Coord. Chem. Rev. 256 (2012) 1556;
(i) J.T.F. Lau, P.C. Lo, W.P. Fong, D.K.P. Ng, J. Med. Chem. 55 (2012) 5446.
[9] (a) T. Nyokong, E. Antunes, in: M.K. Kadish, K.M. Smith, R. Guilard (Eds.), The Handbook of Porphyrins Science, vol. 7, Academic Press, World Scientific Singapore, New York, 2010, p. 247 (Chapter 34);
(b) T. Nyokong, Pure Appl. Chem. 83 (2011) 1763;
(c) C. Tanielian, C. Wolff, J. Phys. Chem. 99 (1995) 9825;
(e) E.D. Sternberg, D. Dolphin, C. Brückner, Tetrahedron 54 (1998) 4151;
(d) W. Shi-Kang, Z. Hou-Chen, C. Guo-Zhu, X. Da-Nian, X. Hui-Jun, Acta Chim. Sin. 3 (1985) 21.
[10] (a) S. Mitra, T.H. Foster, Biophys. J. 78 (2000) 2597;
(b) M. Prein, W. Adam, Angew. Chem., Int. Ed. Engl. 35 (1996) 477;
(c) M.R. Badger, S. Caemmererm, S. Ruuska, H. Nakano, Phil. Trans. R. Soc. London B 355 (2000) 1433;
(d) D.R. Ort, N.R. Baker, Curr. Opin. Plant Biol. 5 (2002) 193.
[11] S. Aronoff, G. Mickinney, J. Am. Chem. Soc. 65 (1943) 956.
[12] (a) H.C. Fry, P.G. Hoertz, L.M. Wasser, K.D. Karlin, G.J. Meyer, J. Am. Chem. Soc. 126 (2004) 16712;
(b) J.P. Collman, I.M. Shiryaevam, R. Boulatov, Inorg. Chem. 42 (2003) 4807;
(c) W. Nam, I. Kim, M.H. Lim, H.J. Choi, J.S. Lee, H.G. Jang, Chem. Eur. J. 8 (2002) 2067;
(d) K. Szaciłowski, A. Chmura, Z. Stasicka, Coord. Chem. Rev. 249 (2005) 2408;
(e) M.W. Makinen, A.K. Churg, H.A. Glick, Proc. Natl. Acad. Sci. USA 75 (1978) 2291.
[13] (a) R. Hückelhoven, K.H. Kogel, Planta 216 (2003) 891;
(b) D.I. Resser, C. George, D.J. Donaldson, J. Phys. Chem. A 113 (2009) 8591;
(c) J. Torrie, C.I. Mayfield, W.E. Inniss, J. Microbiol. Methods 6 (1987) 199;
(d) E. Kessler, Planta (Berl.) 92 (1970) 222;
(e) J.J. Katz, Naturwissenschaften 60 (1973) 32.
[14] R. Kubiak, J. Janczak, M. Śledź, E. Bukowska, Polyhedron 27 (2008) 3044.
[15] CRYSALIS CCD and CRYSALIS Red Program, Ver. 171.31.8, Oxford Diffraction Poland, Wrocław, Poland, 2006.
[16] G.M. Sheldrick, SHELXS97, SHELXL97, Programs for Crystal Structure Solution and Refinement, University of Göttingen, Göttingen, Germany, 1997.
[17] A.L. Spek, PLATON, Utrecht University, The Netherlands, 2005.
[18] K. Brandenburg, H. Putz, DIAMOND, Ver. 3.0, Crystal and Molecular Structure Visualization, University of Bonn, Germany, 2006.
[19] WINXPOW Software Manual, STOE & GmbH, Darmstadt, Germany, 1997.
[20] J.M. Frisch, G.W. Trucks, H.B. Schlegel, M.A. Robb, J. Cheeseman, T. Keith, G.A. Petersson, J.A. Montgomery Jr., T. Vreven, K.N. Kudin, J.C. Burant, J.M. Millam, S.S. Iyengar, J. Tomasi, V. Barone, B. Mennucci, M. Cossi, G. Scalmani, N. Rega, G.A. Petersson, H. Nakatsuji, M. Hada, M. Ehara, K. Toyota, R. Fukuda, J. Hasegawa, M. Ishida, T. Nakajima, Y. Honda, O. Kiato, H. Nakani, M. Klene, X. Li, J.E. Knox, H.P. Hratchian, J.B. Cross, V. Bakken, C. Adamo, J. Jaramillo, R. Comperts, R.E. Stratmann, P. Yazyev, A.J. Austin, R. Cammi, C. Pomelli, J.W. Ochterski, P.Y. Ayala, K. Morokuma, G.A. Voth, P. Salvador, J.J. Dannenberg, V.G. Zakrzewski, S. Dapprich, A.D. Daniels, M.C. Strain, O. Frakas, D.K. Malick, A.D. Rabuck, K. Raghavachari, J.B. Foresman, J.V. Ortiz, Q. Cui, A.G. Baboul, S. Clifford, J. Cislowski, B.B. Stefanov, G. Liu, A. Liashenko, A. Piskorz, I. Komaromi, R.L. Martin, D.J. Fox, T. Keith, M.A. Al-Laham, C.J. Peng, A. Nanayakkara, M. Challacombe, P.M.W. Gill, B. Johnson, W. Chen, M.W. Wong, C. Gonzales, J.A. Pople, GAUSSIAN03, Revision D.01, Programme, Gaussian, Inc., Wallingford, CT, 2004.
[21] (a) A.D. Becke, J. Chem. Phys. 104 (1996) 1040;
(b) C. Lee, W. Yang, R.G. Parr, Phys. Rev. B 37 (1988) 785.
[22] B.G. Parr, W. Yang, Density-Functional Theory of Atoms and Molecules, Oxford University Press, New York, 1989.
[23] (a) J. Janczak, Polyhedron 29 (2010) 941;
(b) V. Kinzhybalo, J. Janczak, J. Mol. Struct. 921 (2009) 1;
(c) V. Kinzhybalo, J. Janczak, Acta Crystallogr., Sect. C 63 (2007) m357;
(d) R. Kubiak, A. Waśkowska, A. Pietraszko, E. Bukowska, Inorg. Chim. Acta 358 (2005) 453;
(e) I.A. Guzei, R.W. McGaff, H.M. Kieler, Acta Crystallogr., Sect. C 61 (2005) m472;
(f) J. Janczak, Y.M. Idemori, Polyhedron 22 (2003) 1167;
(g) S. Matsumoto, A. Endo, J. Mizuguchi, Z. Kristallogr. 215 (2000) 182.
[24] (a) H. Tomoda, S. Saito, S. Ogawa, S. Shiraishi, Chem. Lett. 12 (1983) 313;
(b) D. Wöhrle, G. Schnurpfeil, G. Knothe, Dyes Pigments 18 (1992) 91;
(c) A.G. Gürek, O. Bekaroglu, J. Chem. Soc., Dalton Trans. (1994) 1419;
(d) K. Ban, K. Nishizawa, K. Ohta, H. Shirai, J. Mater. Chem. 10 (2000) 1083.
[25] J. Janczak, Polyhedron 30 (2011) 2933.
[26] (a) C. Kartky, J.D. Dunitz, Acta Crystallogr., Sect. B 31 (1975) 1586;
(b) H.C. Chow, R. Serlin, C.E. Strouse, J. Am. Chem. Soc. 97 (1975) 7230;
(c) R. Serlin, H.C. Chow, C.E. Strouse, J. Am. Chem. Soc. 97 (1975) 7237.
[27] (a) E. Ough, Z. Gasyna, M.J. Stillman, Inorg. Chem. 30 (1991) 2301;
(b) P. Corbeau, M.T. Riou, C. Clarisse, M. Bardin, V. Plichon, J. Electroanal.

Chem. 274 (1989) 107;
(c) H. Sugimoto, T. Higashi, M. Mori, Chem. Lett. 8 (1983) 1167;
(d) A.T. Chang, J.C. Marchon, Inorg. Chim. Acta 53 (1981) L241.
[28] J. Janczak, R. Kubaik, J. Lisowski, Polyhedron 30 (2011) 253.
[29] R.J. Gillespie, Chem. Soc. Rev. 23 (1992) 59.
[30] C. Schweitzer, R. Schmidt, Chem. Rev. 103 (2003) 1685.
[31] (a) P. Sjoberg, P. Politzer, J. Phys. Chem. 94 (1990) 3959;
(b) P. Politzer, J.S. Murray, Comput. Med. Chem. Drug Disc. (2004) 213;
(c) C.A. Hunter, Angew. Chem., Int. Ed. 43 (2004) 5310;
(d) A.L. Cashin, E.J. Petersson, H.A. Lester, D.A. Dougherty, J. Am. Chem. Soc. 127 (2005) 350.